

Itaconate and fumarate derivatives exert a dual inhibitory effect on canonical NLRP3 activation in macrophages and microglia

1 **Christopher Hoyle*, Jack P Green, Stuart M Allan, David Brough*, Eloise Lemarchand**

2 Geoffrey Jefferson Brain Research Centre, The Manchester Academic Health Science Centre,

3 Northern Care Alliance NHS Group, University of Manchester

4 Division of Neuroscience and Experimental Psychology, School of Biological Sciences, Faculty of
5 Biology, Medicine and Health, University of Manchester, AV Hill Building, Manchester, UK

6 The Lydia Becker Institute of Immunology and Inflammation, University of Manchester, AV Hill
7 Building, Manchester, UK

8 *** Corresponding authorship:**

9 Christopher Hoyle

10 christopher.hoyle@manchester.ac.uk

11 ORCID iD: <https://orcid.org/0000-0002-2075-303X>

12 David Brough

13 david.brough@manchester.ac.uk

14 ORCID iD: <https://orcid.org/0000-0002-2250-2381>

15

16 **Keywords: itaconate, fumarate, NLRP3, inflammasome, interleukin-1 β , macrophage,
17 microglia, organotypic hippocampal slice culture**

18 **Summary statement**

19 We show that itaconate and fumarate derivatives inhibit both the priming and activation steps of
20 NLRP3 inflammasome responses in macrophages and microglia, revealing the importance of
21 immunometabolic NLRP3 regulation.

22 Abstract

23 The NLRP3 inflammasome is a multi-protein complex that regulates the protease caspase-1 and
24 subsequent interleukin (IL)-1 β release from cells of the innate immune system, or microglia in the
25 brain, in response to infection or injury. Derivatives of the metabolites itaconate and fumarate, dimethyl
26 itaconate (DMI), 4-octyl itaconate (4OI) and dimethyl fumarate (DMF), limit both expression of IL-1 β ,
27 and IL-1 β release following NLRP3 inflammasome activation. However, the direct effects of these
28 metabolite derivatives on NLRP3 inflammasome responses in macrophages and microglia require
29 further investigation. Using murine bone marrow-derived macrophages, mixed glia and organotypic
30 hippocampal slice cultures (OHSCs), we demonstrate that DMI and 4OI pre-treatment limited IL-1 β ,
31 IL-6 and tumor necrosis factor production in response to lipopolysaccharide (LPS) priming, as well as
32 inhibiting subsequent NLRP3 inflammasome activation. DMI, 4OI, DMF and monomethyl fumarate
33 (MMF), another fumarate derivative, also directly inhibited biochemical markers of NLRP3 activation
34 in LPS-primed macrophages, mixed glia and OHSCs, including ASC speck formation, caspase-1
35 activation, gasdermin D cleavage and IL-1 β release. Finally, DMF, an approved treatment for multiple
36 sclerosis, as well as DMI, 4OI and MMF, inhibited NLRP3 activation in macrophages in response to
37 the phospholipid lysophosphatidylcholine, which is used to induce demyelination, suggesting a
38 possible mechanism of action for DMF in multiple sclerosis through NLRP3 inhibition. Together, these
39 findings reveal the importance of immunometabolic regulation for both the priming and activation
40 steps of NLRP3 activation in macrophages and microglia. Furthermore, we highlight itaconate and
41 fumarate derivatives as a potential therapeutic option in NLRP3-driven diseases, including in the brain.

42 1 Introduction

43 Macrophages are innate immune effector cells that regulate inflammatory responses upon infection or
44 tissue injury to restore tissue homeostasis by promoting pathogen death or tissue and wound repair. In
45 the brain, macrophage-like cells called microglia are important effectors of this inflammatory response.
46 Inflammasomes are cytosolic complexes that regulate the inflammatory response in immune cells and
47 microglia. In particular, the nucleotide-binding oligomerisation domain-, leucine-rich repeat- and pyrin
48 domain-containing protein 3 (NLRP3) inflammasome has been implicated in a range of non-
49 communicable diseases that are characterised by an inflammatory response (Chen and Nuñez, 2010;
50 Rock et al., 2010). Although several pathways of NLRP3 activation have been described (Gaidt et al.,
51 2016; Kayagaki et al., 2011), canonical NLRP3 activation is the most studied. The canonical pathway
52 consists of an initial priming step, typically mediated through Toll-like receptor signaling, that
53 upregulates NLRP3 and IL-1 β expression, followed by a subsequent NLRP3 activating stimulus. A
54 broad range of pathogen- or damage-associated molecular patterns are known to act as this activating
55 stimulus, including the potassium ionophore nigericin, extracellular ATP (Perregaux and Gabel, 1994),
56 amyloid- β aggregates (Halle et al., 2008) or silica crystals (Dostert et al., 2008; Hornung et al., 2008).
57 The precise mechanism by which these stimuli induce NLRP3 activation is still unclear, with potassium
58 efflux-dependent (Muñoz-Planillo et al., 2013) and -independent (Groß et al., 2016) mechanisms
59 suggested to elicit dispersal of the trans-Golgi network, leading to inflammasome formation (Chen and
60 Chen, 2018). We recently proposed organelle dysfunction to be a crucial cellular event that leads to
61 NLRP3 activation (Seoane et al., 2020). Once activated, NLRP3 interacts with the adaptor protein ASC
62 (apoptosis-associated speck-like protein containing a caspase recruitment domain), causing the
63 formation of an ASC speck that drives activation of the inflammasome effector protein caspase-1
64 (Boucher et al., 2018; Schroder and Tschopp, 2010). Active caspase-1 then cleaves gasdermin D and
65 pro-interleukin (IL)-1 β , with gasdermin D pores potentially forming the conduit for mature IL-1 β
66 release (He et al., 2015).

67 Immunometabolism has emerged as a regulator of macrophage inflammasome responses (O'Neill and
68 Artyomov, 2019). Lipopolysaccharide (LPS) treatment of macrophages causes a metabolic shift from
69 oxidative phosphorylation to glycolysis that is necessary for IL-1 β production (Tannahill et al., 2013).
70 Certain metabolites such as itaconate (O'Neill and Artyomov, 2019), succinate (Mills and O'Neill,
71 2014) and fumarate (Humphries et al., 2020) have immunoregulatory functions. For example, itaconate
72 and fumarate derivatives, including dimethyl itaconate (DMI), 4-octyl itaconate (4OI) and dimethyl

73 fumarate (DMF), are able to activate nuclear factor erythroid 2-related factor 2 (NRF2) signalling by
74 alkylating and subsequently inducing the degradation of the cytoplasmic NRF2 inhibitor kelch-like
75 ECH-associated protein 1 (KEAP1) (Mills et al., 2018). NRF2 is then able to translocate to the nucleus,
76 where it not only upregulates the transcription of its target genes, but also prevents the recruitment of
77 RNA polymerase II to NF- κ B secondary response genes such as IL-6 and IL-1 β (Kobayashi et al.,
78 2016). DMI and 4OI also induce electrophilic stress and glutathione depletion in macrophages, which
79 inhibits the LPS-induced translation of I κ B ζ independently of NRF2, and this subsequently limits the
80 expression of I κ B ζ -dependent NF- κ B secondary response genes (Bambouskova et al., 2018; Swain et
81 al., 2020). It must be acknowledged that the properties of these itaconate derivatives may not fully
82 reflect the properties of endogenous itaconate (Swain et al., 2020). *In vivo* evidence also indicates the
83 importance of itaconate responses, as mice deficient in *Irg1*, which therefore cannot produce itaconate,
84 rapidly succumb to *Mycobacterium tuberculosis* infection, whereas there was no mortality in wild-type
85 control mice (Nair et al., 2018). Interestingly, 4OI and DMF exhibit anti-viral and anti-inflammatory
86 effects through NRF2 signalling in response to Severe Acute Respiratory Syndrome Coronavirus 2
87 (SARS-CoV2) infection (Olagnier et al., 2020).

88 Although itaconate derivatives are known to limit IL-1 β expression, the direct effects of itaconate-
89 related compounds on NLRP3 inflammasome activation are less characterized. Previous studies
90 suggest that DMF, an approved treatment for relapsing-remitting multiple sclerosis, and its metabolite
91 monomethyl fumarate (MMF), limit NLRP3 inflammasome activation, with DMF exhibiting greater
92 potency (Liu et al., 2016; Miglio et al., 2015). DMF has also been shown to directly succinate a cysteine
93 residue on gasdermin D to limit pyroptotic cell death in response to NLRP3 activation *in vitro* and *in*
94 *vivo*, but without inhibiting NLRP3 activation itself (Humphries et al., 2020). Itaconate and its
95 derivative 4OI can inhibit NLRP3 activation in an NRF2-independent manner, through the
96 modification of specific cysteine residues on NLRP3, which may prevent NLRP3's interaction with
97 NEK7 and subsequent activation (Hooftman et al., 2020; Swain et al., 2020). IRG1-deficient
98 macrophages, which cannot synthesize endogenous itaconate, exhibit enhanced IL-1 β release in
99 response to NLRP3 inflammasome activation. Finally, 4OI is effective at inhibiting NLRP3 activation
100 *in vivo* (Hooftman et al., 2020).

101 Despite recent advances, further characterisation of the effects of itaconate- and fumarate-related
102 compounds on NLRP3 inflammasome activation is required in order to evaluate their therapeutic
103 potential. The relevance of immunometabolic regulation of microglial inflammasome responses in the

104 brain is also unclear. Here, we demonstrate that itaconate derivative pre-treatment not only prevented
105 expression of IL-1 β , but also inhibited canonical NLRP3 inflammasome activation. We identified that
106 itaconate and fumarate derivatives were able to directly inhibit canonical NLRP3 inflammasome
107 activation, independent of their inhibitory effect on priming. These effects were consistent in mixed
108 glia and organotypic hippocampal slice cultures (OHSCs), two brain-relevant NLRP3 inflammasome
109 models (Hoyle et al., 2020). Finally, itaconate and fumarate derivatives inhibited NLRP3 activation
110 induced by lysophosphatidylcholine (LPC), a lipid molecule used to induce demyelination in models
111 of multiple sclerosis, further highlighting a potential mechanism of DMF action in multiple sclerosis
112 treatment. These findings reveal a dual anti-inflammatory effect of itaconate and fumarate derivatives
113 in the innate immune system and brain, through regulation of both the priming and activation steps of
114 canonical NLRP3 inflammasome responses.

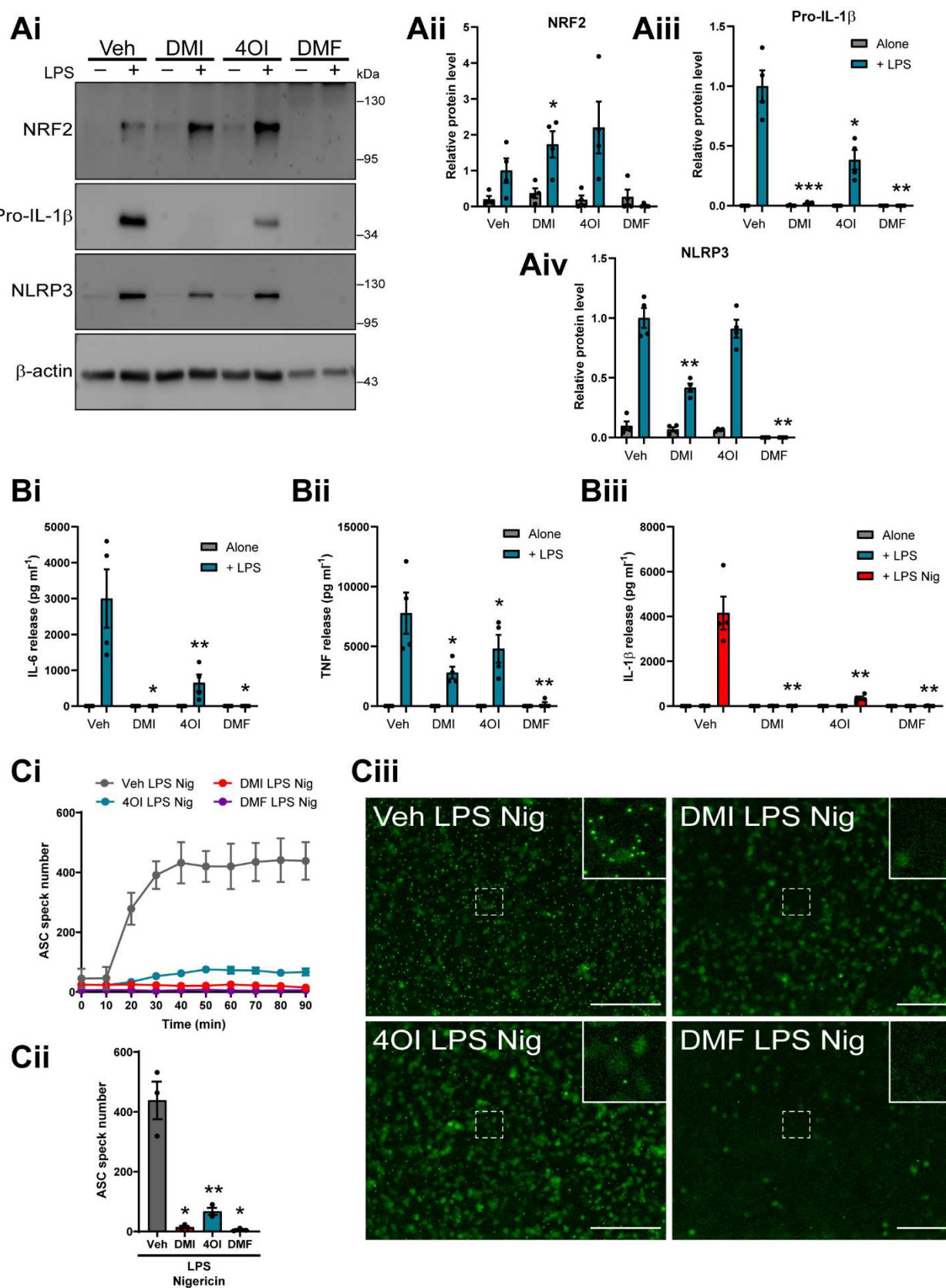
115

116 2 Results

117 *Pre-treatment with itaconate and fumarate derivatives reduces NLRP3 priming and canonical*
118 *inflammasome activation*

119 BMDMs were pre-treated with two cell-permeable derivatives of itaconate, DMI and 4OI, as well as
120 the fumarate derivative DMF, and the effects on NLRP3 priming and activation were assessed. DMI
121 and 4OI treatment alone did not induce NRF2 accumulation in murine WT BMDMs, but both enhanced
122 LPS-induced NRF2 accumulation (Figure 1A). DMF treatment was toxic to the cells at this treatment
123 duration and concentration, explaining the lack of NRF2 accumulation (Figure 1A, Supplementary
124 Figure 1). I κ B ζ protein levels were not measured. DMI and 4OI pre-treatment inhibited the production
125 of pro-IL-1 β in response to LPS priming, and whilst DMI reduced NLRP3 expression to a lesser extent,
126 4OI had no effect on NLRP3 levels (Figure 1A). No pro-IL-1 β or NLRP3 protein was observed
127 following DMF pre-treatment, although this was probably due to toxicity prior to LPS priming (Figure
128 1A, Supplementary Figure 1). DMI and 4OI also strongly reduced LPS-induced IL-6 release, with a
129 smaller reduction in TNF release (Figure 1Bi, Bii). Consistent with inhibition of pro-IL-1 β expression,
130 DMI and 4OI pre-treatment blocked IL-1 β release in response to subsequent stimulation with LPS and
131 nigericin (Figure 1Biii). These data confirmed previous findings that itaconate derivative treatment
132 prior to LPS stimulation could limit inflammatory priming via NRF2 activation (Mills et al., 2018).

133 We next investigated whether itaconate derivative pre-treatment could reduce NLRP3 inflammasome
134 activation, as has been recently suggested (Swain et al., 2020). Treatment of murine BMDMs from
135 ASC-citrine reporter mice (Tzeng et al., 2016) with DMI, 4OI and DMF prior to LPS priming inhibited
136 the formation of ASC specks upon subsequent nigericin treatment (Figure 1Ci, Cii), with representative
137 images from this experiment after 90 minutes of nigericin treatment shown (Figure 1Ciii).
138 Morphological changes due to nigericin treatment are also shown using bright-field microscopy
139 (Supplementary Figure 1). DMF pre-treatment induced a high level of cell toxicity, perhaps explaining
140 its strong inhibitory effect on NLRP3 inflammasome formation and IL-1 β release. These data
141 suggested that itaconate derivative pre-treatment may additionally inhibit the NLRP3 inflammasome
142 activation step, as well as inhibiting the priming stage.

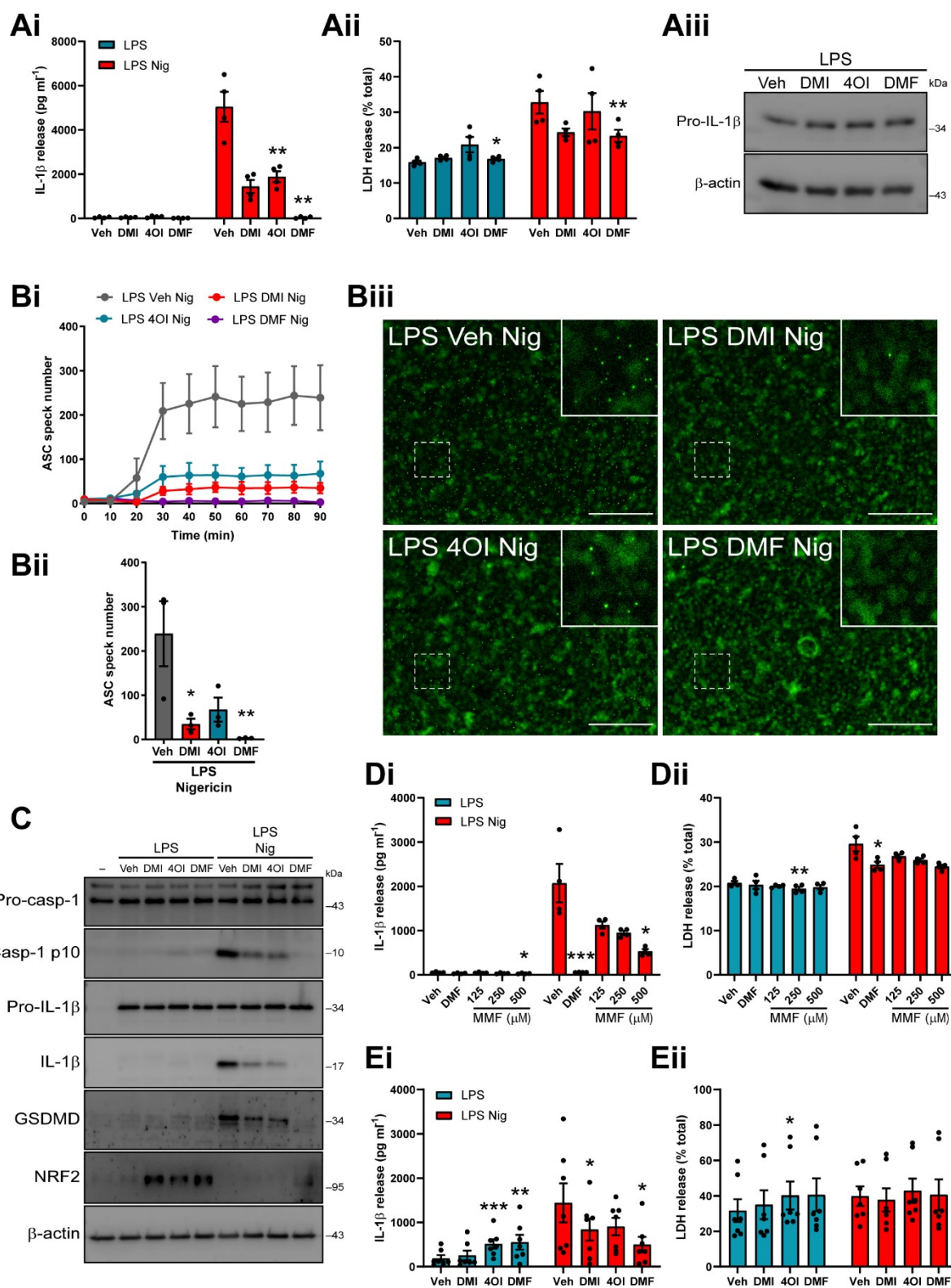


144 **Figure 1. Pre-treatment with itaconate and fumarate derivatives reduces NLRP3 priming and**
145 **canonical inflammasome activation. (A)** WT BMDMs were treated with vehicle (DMSO), DMI, 4OI
146 or DMF (125 μ M, 20 h). LPS (1 μ g ml⁻¹, 4 h) was then added to the wells to induce priming (n=4).
147 **(Ai)** Cell lysates were probed by western blotting for NRF2, pro-IL-1 β and NLRP3 protein, and **(Aii-iv)**
148 densitometry was performed on each independent experiment (expressed relative to Veh+LPS
149 treatment). **(B)** WT BMDMs were treated as above, followed by nigericin (10 μ M, 60 min; n=4).
150 Supernatants were assessed for **(Bi)** IL-6, **(Bii)** TNF and **(Biii)** IL-1 β content by ELISA. **(C)** ASC-
151 citrine BMDMs were treated as above, followed by nigericin (10 μ M, 90 min; n=3). ASC speck
152 formation was measured over a period of 90 min. Image acquisition began immediately after addition
153 of nigericin. **(Ci)** ASC speck number per field of view was quantified over 90 min. **(Cii)** ASC speck
154 number and **(Ciii)** fluorescence images after 90 min nigericin treatment are shown. Scale bars are 200
155 μ m. Data are presented as mean \pm SEM. Data were analysed using repeated-measures one-way (Cii)
156 or two-way (Aii-iv, B) ANOVA with Dunnett's post-hoc test (versus Veh treatment within each
157 group). *P<0.05; **P<0.01, ***P<0.001.

158 *Itaconate and fumarate derivatives directly inhibit the NLRP3 activation step*

159 To determine whether NLRP3 inflammasome inhibition was a direct effect of the itaconate derivatives,
160 LPS-primed WT BMDMs were treated with DMI, 4OI and DMF prior to nigericin stimulation, and
161 this resulted in inhibition of IL-1 β release, as well as small reductions in cell death (Figure 2Ai, Aii).
162 Western blotting of the cell lysates demonstrated that the levels of pro-IL-1 β were consistent between
163 treatments, confirming that in this protocol expression of pro-IL-1 β was unaffected by DMI, 4OI or
164 DMF (Figure 2Aiii, Supplementary Figure 2A). Dose-dependent inhibition of IL-1 β release was
165 observed for each treatment, with minimal reductions in cell death (Supplementary Figure 3). ASC
166 speck formation was measured in LPS-primed ASC-citrine BMDMs treated with DMI, 4OI and DMF
167 prior to nigericin. Each of these metabolite derivatives inhibited ASC speck formation in response to
168 nigericin, suggesting that these compounds were also able to directly block NLRP3 inflammasome
169 activation independently of their effects on the priming response (Figure 2Bi-iii). Fluorescence and
170 bright-field images are shown (Figure 2Bi, Supplementary Figure 4). DMF treatment after LPS priming
171 did not induce morphologically observable cell death, indicating that DMF was able to inhibit NLRP3
172 inflammasome activation independent of toxicity at this concentration and duration of incubation, and
173 this has been reported previously (Garstkiewicz et al., 2017; Liu et al., 2016; Miglio et al., 2015)
174 (Supplementary Figure 3). LPS-primed primary BMDMs treated with DMI, 4OI or DMF and
175 subsequent nigericin stimulation were lysed directly in-well without removing the supernatant, and
176 western blotting confirmed reductions in caspase-1 activation, and gasdermin D and IL-1 β cleavage
177 (Figure 2C, Supplementary Figure 2B). NRF2 levels were increased by DMI, 4OI and DMF treatment
178 after LPS priming, although this was not observed in cells that received subsequent nigericin

179 stimulation (Figure 2C, Supplementary Figure 2B), and itaconate-mediated NLRP3 inhibition is
180 suggested to be independent of NRF2 (Hooftman et al., 2020; Swain et al., 2020). MMF treatment
181 limited NLRP3 activation in LPS-primed BMDMs, although it was not as potent as DMF (Fig 2Di,
182 Dii). We confirmed that exogenous itaconate treatment also inhibited NLRP3 activation in LPS-primed
183 BMDMs, although much higher doses were required because it is less cell permeable (Supplementary
184 Figure 5) (Swain et al., 2020). To determine whether the inhibitory effects of itaconate and fumarate
185 derivatives were relevant in human macrophages, LPS-primed human MDMs were treated with DMI,
186 4OI and DMF prior to nigericin stimulation. 4OI and DMF alone appeared to induce IL-1 β release,
187 although slight increases in cell death were observed for these treatments, which may have allowed
188 passive release of unprocessed pro-IL-1 β (Figure 2Ei). Both DMI and DMF reduced nigericin-induced
189 IL-1 β release, whereas 4OI did not significantly reduce IL-1 β release at this dose (Figure 2Ei). No
190 inhibition of cell death was observed (Figure 2Eii). Thus, the itaconate and fumarate derivatives were
191 able to directly inhibit NLRP3 activation in peripheral macrophages, independent of their effects on
192 priming.



193

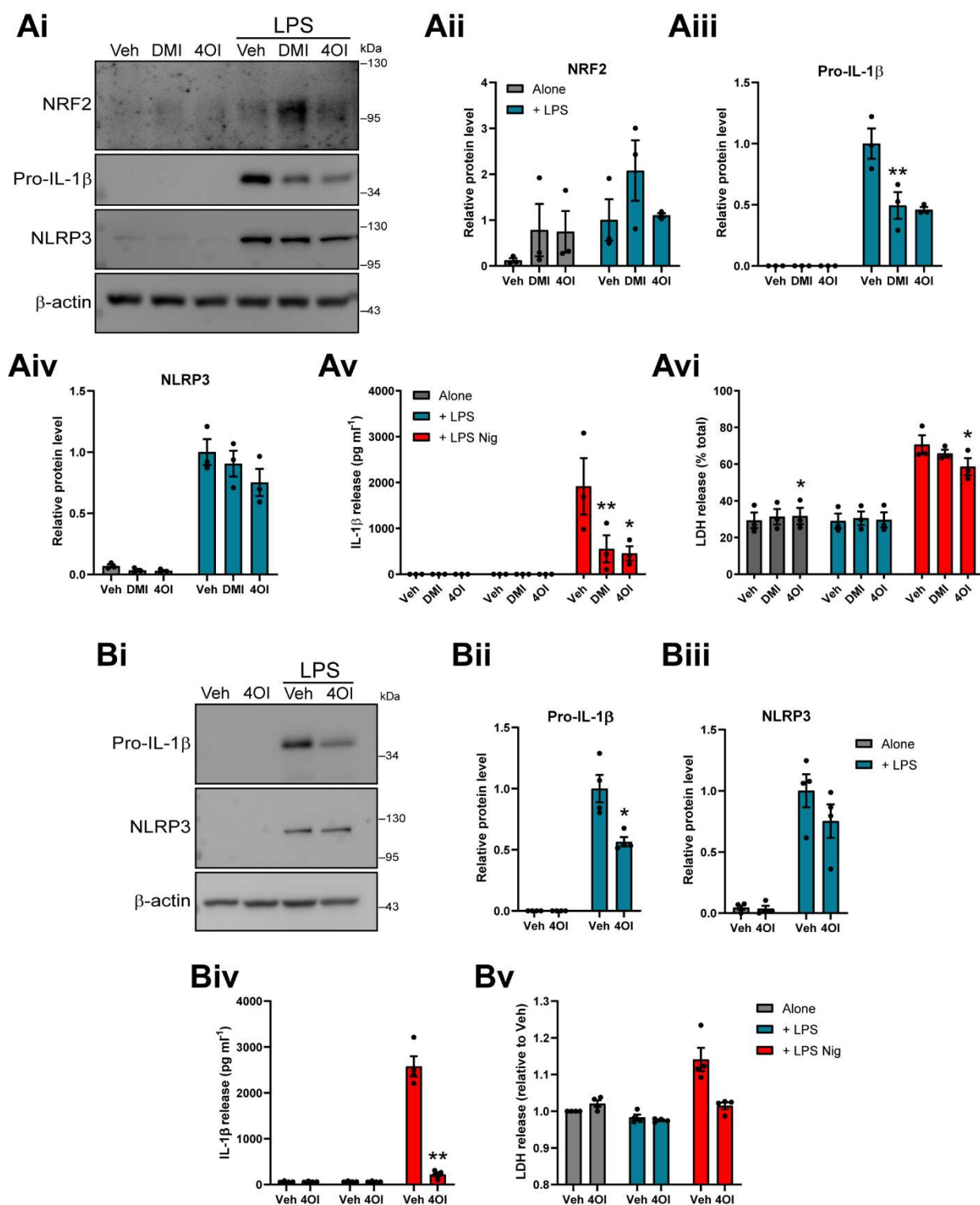
194 **Figure 2. Itaconate and fumarate derivatives directly inhibit the NLRP3 activation step in**
195 **murine and human macrophages. (A) WT BMDMs were primed with LPS (1 μg ml⁻¹, 4 h) before**
196 **treatment with vehicle (DMSO), DMI, 4OI or DMF (125 μM, 15 min). Nigericin was then added to**

197 the well (10 μ M, 60 min; n=4). Supernatants were assessed for (Ai) IL-1 β release and (Aii) cell death
198 (LDH release). (Aiii) Cell lysates were probed by western blotting for pro-IL-1 β protein. See
199 Supplementary Figure 2A. (B) ASC–citrine BMDMs were treated as above, and ASC speck formation
200 was measured over a period of 90 min (n=3). Image acquisition began immediately after addition of
201 nigericin. (Bi) ASC speck number per field of view was quantified over 90 min. (Bii) ASC speck
202 number and (Biii) fluorescence images after 90 min nigericin treatment are shown. Scale bars are 200
203 μ m. (C) WT BMDMs were treated as above and then lysed in-well and probed for several markers of
204 inflammasome activation by western blotting (n=4). See Supplementary Figure 2B. (D) WT BMDMs
205 were LPS primed (1 μ g ml $^{-1}$, 4 h) before treatment with vehicle (DMSO), DMF (125 μ M) or MMF
206 (125–500 μ M, 15 min). Nigericin was then added to the well (10 μ M, 60 min; n=4). Supernatants were
207 assessed for (Di) IL-1 β release and (Dii) LDH release. (E) Human MDMs were LPS primed (1 μ g ml $^{-1}$,
208 4 h) before treatment with vehicle (DMSO), DMI, 4OI or DMF (125 μ M, 15 min). Nigericin was
209 then added to the well (10 μ M, 60 min; n=7). Supernatants were assessed for (Ei) IL-1 β release and
210 (Eii) LDH release. Supernatants were assessed for cytokine content by ELISA. Data are presented as
211 mean \pm SEM. Data were analysed using repeated-measures one-way (Bii) or two-way (Ai, Aii, D, E)
212 ANOVA with Dunnett's post-hoc test (versus Veh treatment within each group). *P<0.05; **P<0.01;
213 ***P<0.001.

214 *Itaconate and fumarate derivatives inhibit NLRP3 priming and canonical activation in mixed glia
215 and OHSCs*

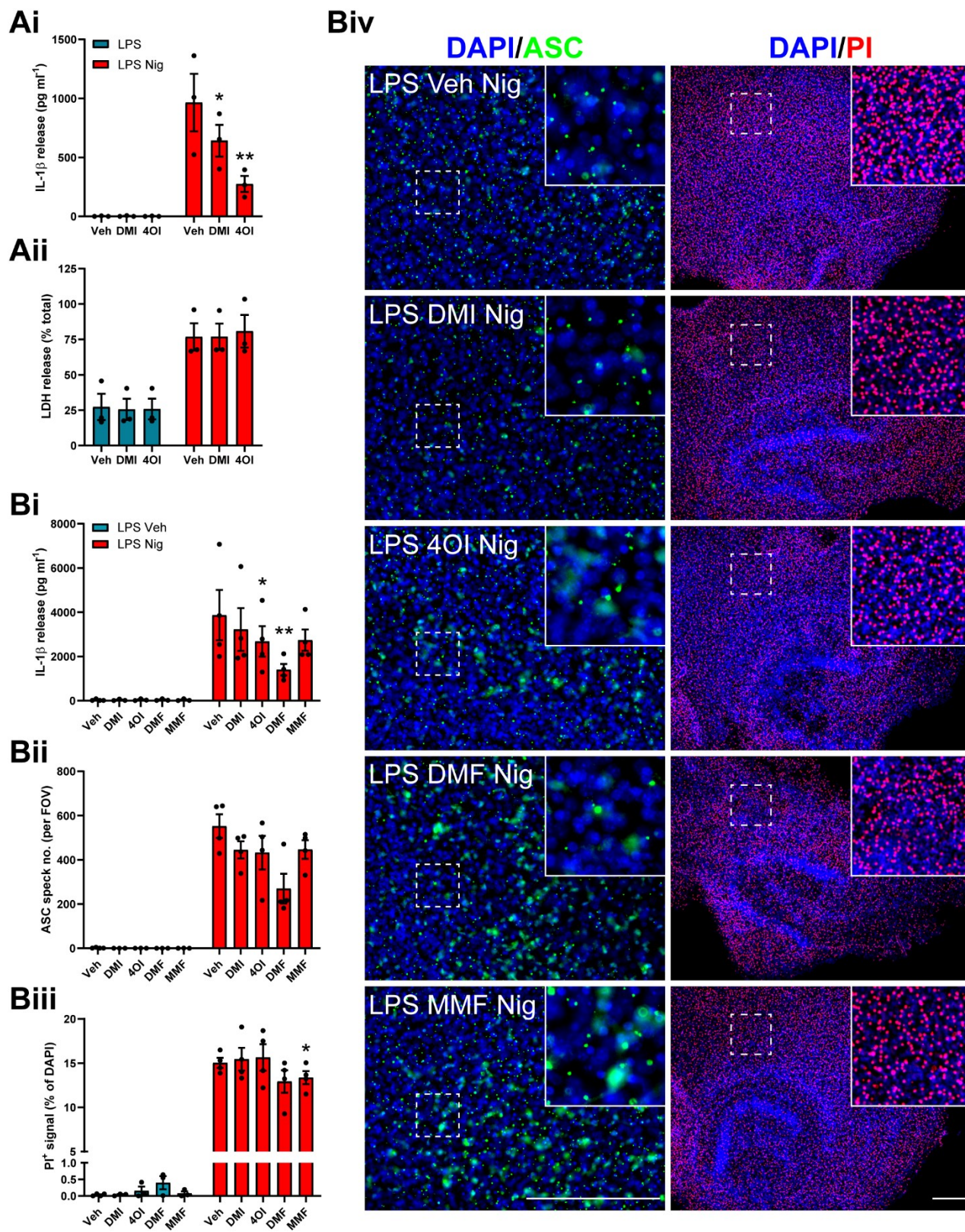
216 Despite accumulating evidence in peripheral immune cells, little is known about the importance of
217 immunometabolic regulation of inflammasome priming and activation in the brain, where microglia
218 are thought to be the predominant source of inflammasomes (Sheppard et al., 2019). Thus, we assessed
219 the effect of itaconate derivative pre-treatment on mixed glial cultures, which consist of approximately
220 80% astrocytes, 10% microglia and 10% oligodendrocyte/type-2 astrocyte progenitor cells (Pinteaux
221 et al., 2002), and organotypic hippocampal slice cultures (OHSCs), which we recently validated as a
222 model for studying microglial NLRP3 responses (Hoyle et al., 2020). DMF was not included in these
223 pre-treatment experiments due to its toxicity observed in murine BMDMs (Figure 1, Supplementary
224 Figure 1), although it has been previously demonstrated to inhibit IL-1 β , IL-6, and to a lesser extent
225 TNF expression at a lower dose in rat neonatal microglial cultures (Wilms et al., 2010). DMI and 4OI
226 alone did not induce detectable NRF2 accumulation in mixed glial cultures (Figure 3Ai, Aii). DMI
227 treatment did not significantly enhance LPS-induced NRF2 accumulation, although increases were
228 observed; similarly, 4OI did not increase LPS-induced NRF2 levels (Figure 3Ai, Aii). I κ B ζ protein
229 levels were not measured. Despite this, both DMI and 4OI reduced pro-IL-1 β production in mixed glial
230 cultures, without affecting NLRP3 protein levels (Figure 3Ai–iv). IL-1 β release upon subsequent
231 stimulation with nigericin was also inhibited by both derivatives, and 4OI modestly reduced cell death

232 (Figure 3Av, Avi). Given that the inhibition of pro-IL-1 β production and mature IL-1 β release was
233 comparable between DMI and 4OI in mixed glia, only 4OI was used in OHSCs. NRF2 accumulation
234 could not be reliably detected in OHSCs upon LPS priming (data not shown). 4OI reduced the
235 production of pro-IL-1 β in response to LPS priming, but did not affect NLRP3 production (Figure 3Bi–
236 iii). 4OI pre-treatment strongly inhibited IL-1 β release in response to LPS and nigericin treatment and
237 reduced cell death (Figure 3Biv, Bv). These data suggested that itaconate derivatives were able to limit
238 the priming of inflammasome responses, and that this may be a relevant mechanism to regulate
239 microglial inflammatory gene expression.



245 on each independent experiment (expressed relative to Veh + LPS treatment). **(Av, Avi)** WT mixed
246 glia were treated as above, followed by nigericin (10 μ M, 60 min; n=3). Supernatants were assessed
247 for **(Av)** IL-1 β release and **(Avi)** cell death (LDH release). **(B)** WT OHSCs were treated with vehicle
248 (DMSO) or 4OI (125 μ M, 21 h). LPS (1 μ g ml $^{-1}$, 3 h) was then added to the wells to induce priming
249 (n=4). **(Bi)** OHSC lysates were probed by western blotting for pro-IL-1 β and NLRP3 protein, and **(Bii-
250 iii)** densitometry was performed on each independent experiment (expressed relative to Veh+LPS
251 treatment). **(Biv, Bv)** WT OHSCs were treated as above, followed by nigericin (10 μ M, 90 min; n=4).
252 Supernatants were assessed for **(Biv)** IL-1 β release and **(Bv)** LDH release. Supernatants were assessed
253 for cytokine content by ELISA. Data are presented as mean \pm SEM. Data were analysed using repeated-
254 measures two-way ANOVA with Dunnett's (A) or Sidak's (B) post-hoc test (versus Veh treatment
255 within each group). *P<0.05; **P<0.01; ***P<0.001.

256 Given that 4OI appeared to inhibit mature IL-1 β release more strongly than it inhibited pro-IL-1 β
257 production in OHSCs, we investigated whether itaconate and fumarate derivatives could directly limit
258 NLRP3 inflammasome activation in mixed glia and OHSCs. LPS-primed mixed glial cultures were
259 treated with DMI and 4OI prior to nigericin stimulation, and this reduced IL-1 β release but did not
260 inhibit cell death (Figure 4Ai, Aii). Similarly, LPS-primed OHSCs were treated with DMI, 4OI, DMF
261 and MMF prior to nigericin stimulation. The compounds alone did not exhibit any toxicity, although a
262 small increase in cell death was observed in response to DMF treatment, nor did they induce ASC
263 speck formation (Supplementary Figure 6). Following nigericin stimulation, 4OI and DMF
264 significantly inhibited IL-1 β release, though this was not accompanied by significant reductions in
265 ASC speck formation (Figure 4Bi, Bii). Only MMF treatment significantly reduced nigericin-induced
266 cell death, although this reduction was modest (Figure 4Biii). Representative immunofluorescence
267 images are shown (Figure 4Biv). Together, these data suggested that the itaconate and fumarate
268 derivatives could reduce microglial NLRP3 responses.



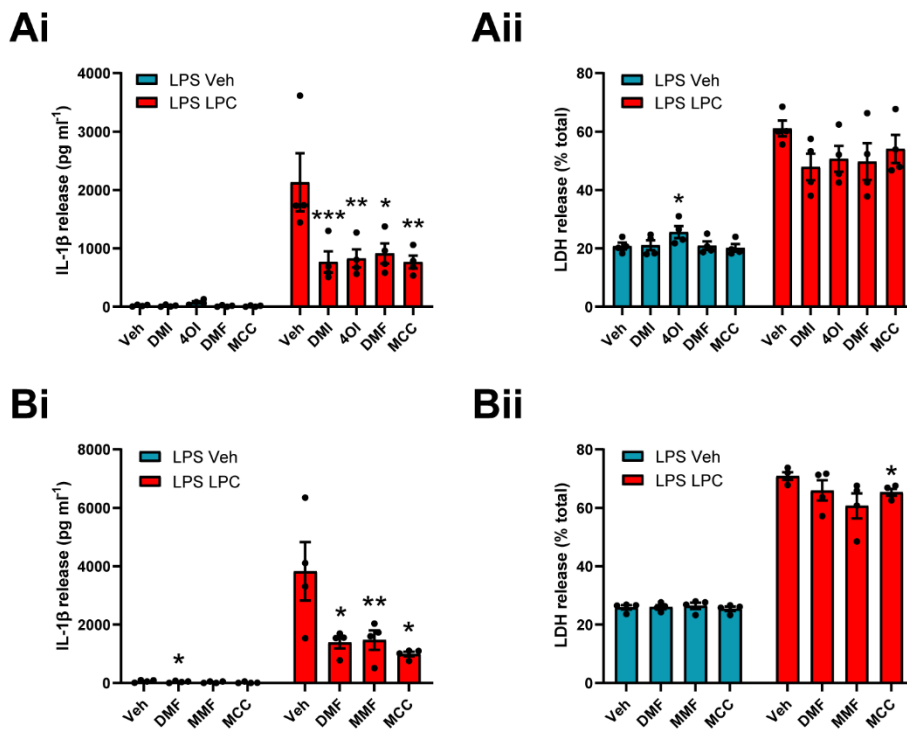
269

270 **Figure 4. Itaconate and fumarate derivatives partly inhibit canonical NLRP3 activation in LPS-
271 primed mixed glia and OHSCs.** (A) Mixed glia were primed with LPS (1 μ g ml $^{-1}$, 3 h) before

272 treatment with vehicle, DMI or 4OI (125 μ M, 15 min). Nigericin was then added to the well (10 μ M,
273 60 min; n=3). Supernatants were assessed for (Ai) IL-1 β release and (Aii) cell death (LDH release).
274 (B) WT OHSCs were primed with LPS (1 μ g ml $^{-1}$, 3 h) before treatment with vehicle (DMSO), DMI,
275 4OI, DMF (125 μ M) or MMF (500 μ M, 15 min). Vehicle (ethanol) or nigericin was then added to the
276 well (10 μ M, 90 min; n=3–4). Propodium iodide (PI; red, 25 μ g ml $^{-1}$) was added for the final 30 min
277 of nigericin treatment. (Bi) Supernatants were assessed for IL-1 β content. OHSCs were probed for
278 nuclei (DAPI, blue) and ASC (green) by immunofluorescence staining. (Bii) ASC speck number per
279 field of view was quantified. (Biii) The area of PI-positive staining was determined and is expressed
280 as a % of total area of DAPI staining. (Biv) Representative images are shown. Images were acquired
281 using widefield microscopy at 20X (ASC) and 5X (PI) magnification. Scale bars are 200 μ m. Data are
282 presented as mean \pm SEM. Data were analysed using repeated-measures two-way ANOVA (A) or
283 mixed effects model (B) with Dunnett's post-hoc test (versus Veh treatment within each group).
284 *P<0.05; **P<0.01.

285 *Itaconate and fumarate derivatives inhibit NLRP3 activation in response to LPC stimulation*

286 LPC (also known as lysolecithin) is a lipid biomolecule that is generated from the cleavage of
287 phosphatidylcholine by phospholipase A₂, or via the action of lecithin-cholesterol acyltransferase (Law
288 et al., 2019). LPC levels are regulated by the enzyme lysophosphatidylcholine acyltransferase, which
289 converts LPC back to phosphatidylcholine (Law et al., 2019). Despite its presence during normal
290 physiology, LPC is able to induce demyelination in experimental models of multiple sclerosis (Hall,
291 1972; Lassmann and Bradl, 2017; Plemel et al., 2018), implicating endogenous LPC dysregulation as
292 a potential factor in multiple sclerosis pathology, although evidence of phospholipase A₂ involvement
293 in multiple sclerosis patients is unclear (Trotter et al., 2019). LPC can also activate the NLRP3 and
294 NLRC4 inflammasomes in macrophages, microglia and astrocytes (Freeman et al., 2017), and NLRP3
295 is reported to be detrimental in experimental autoimmune encephalomyelitis (Coll et al., 2015; Gris et
296 al., 2010; Jha et al., 2010). Thus, LPC-induced NLRP3 inflammasome activation may directly
297 influence LPC-induced demyelination. We assessed whether the itaconate and fumarate derivatives
298 could inhibit NLRP3 activation driven by LPC stimulation in peripheral macrophages. LPS-primed
299 BMDMs were treated with DMI, 4OI, DMF or MCC950, a selective NLRP3 inhibitor (Coll et al.,
300 2015), prior to LPC stimulation. Each of the derivatives inhibited IL-1 β release to the same extent as
301 MCC950, indicating inhibition of NLRP3 activation, although no reductions in cell death were
302 observed by any treatment (Figure 5Ai, Aii). Similarly, treatment with MMF inhibited IL-1 β release
303 induced by LPC to the same extent as MCC950 (Figure 5Bi, Bii). These data suggest that itaconate
304 and fumarate derivatives could limit NLRP3 activation in peripheral macrophages in response to LPC
305 stimulation.



306

307 **Figure 5. Itaconate and fumarate derivatives inhibit NLRP3 activation in response to LPC**
308 **stimulation. (A)** WT BMDMs were primed with LPS ($1 \mu\text{g ml}^{-1}$, 4 h) before treatment with vehicle
309 (DMSO), DMI, 4OI, DMF (125 μM) or MCC950 (10 μM , 15 min). Vehicle (ethanol) or LPC (100
310 μM , 60 min) was then added to the well (n=4). **(B)** WT BMDMs were LPS primed ($1 \mu\text{g ml}^{-1}$, 4 h)
311 before treatment with vehicle (DMSO), DMF (125 μM), MMF (500 μM) or MCC950 (10 μM ,
312 15 min). Vehicle (ethanol) or LPC (100 μM , 60 min) was then added to the well (n=4). Supernatants
313 were assessed for **(AI, BI)** IL-1 β release by ELISA and **(AII, BI)** cell death (LDH release). Data are
314 presented as mean \pm SEM. Data were analysed using repeated-measures two-way ANOVA with
315 Dunnett's post-hoc test (versus Veh treatment within each group). *P<0.05; **P<0.01; ***P<0.001.

316

317 **3 Discussion**

318 Macrophage metabolism has emerged as an important regulator of inflammatory responses (O'Neill
319 and Artyomov, 2019). In particular, exogenous treatment with derivatives of the metabolite itaconate
320 inhibits the expression of NF- κ B secondary response genes such as IL-1 β and IL-6 through NRF2
321 accumulation (Mills et al., 2018) and inhibition of I κ B ζ translation (Bambouskova et al., 2018).
322 However, the direct effect of itaconate derivative treatment on NLRP3 inflammasome activity is
323 unclear, with a few recent studies indicating inhibition of IL-1 β release independently of reductions in
324 pro-IL-1 β (Hooftman et al., 2020; Swain et al., 2020). We confirmed that DMI and 4OI are able to
325 inhibit the expression of pro-inflammatory genes in macrophages upon LPS priming and show that this
326 mechanism may have relevance in microglia. We also found that DMI, 4OI, DMF and MMF can
327 directly inhibit biochemical hallmarks of NLRP3 inflammasome activation independently of their
328 effects on inflammasome priming, including in human macrophages. These findings highlight that
329 itaconate and fumarate derivatives could potentially be manipulated therapeutically in NLRP3-driven
330 diseases, conferring the dual benefit of targeting both priming and activation of NLRP3.

331 Exogenous itaconate has different properties from commonly used itaconate derivatives such as DMI
332 and 4OI, which exhibit greater electrophilicity (Swain et al., 2020). For example, exogenous itaconate
333 does not appear to strongly drive NRF2 signalling, nor does it inhibit I κ B ζ translation, and so any
334 effects of itaconate derivatives, although still relevant, may not directly reflect the physiology of
335 endogenous itaconate (Swain et al., 2020). It has also been shown that DMI is not metabolised to
336 itaconate in the cytosol (ElAzzouny et al., 2017). Nevertheless, whilst itaconate derivatives may not be
337 appropriate to simulate the actions of endogenous itaconate, any therapeutic potential for these
338 compounds maintains importance. Interestingly, Swain et al. (2020) also suggested that itaconate
339 derivatives, including exogenous itaconate, can inhibit NLRP3 activation independently of effects on
340 NRF2 and priming. However, itaconate treatments were only applied prior to LPS priming, instead of
341 treating LPS-primed BMDMs with itaconate prior to NLRP3 activation. Thus, it remains possible that
342 other effects of itaconate pre-treatment, such as reduction in NLRP3 protein levels during LPS priming,
343 could have limited IL-1 β release. We have addressed this in the current study, complementing
344 observations that 4OI specifically inhibited NLRP3 activation in LPS-primed cells through direct
345 interaction with cysteine 548 on murine NLRP3, preventing NEK7 binding (Hooftman et al., 2020).
346 This mechanism is plausible, given that DMI, 4OI and DMF are electrophiles that modify cysteine
347 residues on target proteins including KEAP1 (Linker et al., 2011; Mills et al., 2018), GAPDH

348 (Kornberg et al., 2018; Liao et al., 2019), and more than a thousand other proteins in LPS-primed RAW
349 macrophages (Qin et al., 2020).

350 We suggest that the inhibitory mechanisms of itaconate and fumarate derivatives on NLRP3 priming
351 and canonical activation may be consistent in microglia. Thus, the implications of immunometabolic
352 regulation of inflammasome responses in the brain should be explored further, particularly in the
353 context of brain pathology. Transcriptomic databases indicate that microglia exhibit relatively high
354 expression of *Nfe2l2* (NRF2) and *Keap1* (Schaum et al., 2018; Zhang et al., 2014). The itaconate-
355 synthesising enzyme *Irg1* (also known as *Acod1*) was recently shown to be upregulated in response to
356 LPS treatment in OHSCs (Chausse et al., 2020), driving subsequent itaconate production, and this was
357 prevented by microglial depletion, indicating that this is primarily a microglial response. Furthermore,
358 exogenous treatment with 4OI limited LPS-induced IL-6 production but did not affect TNF (Chausse
359 et al., 2020). While mixed glia and OHSCs are useful tools to study microglial function, further studies
360 are required to fully understand the physiological relevance of microglial metabolic reprogramming *in*
361 *vivo*. NRF2 activation is associated with a protective effect in experimental ischaemic stroke models
362 (Liu et al., 2019), and IRG-deficient mice exhibit exacerbated brain damage to acute ischaemic stroke,
363 according to a recent pre-print (Kuo et al., 2020b). These studies suggest that itaconate production
364 could be an endogenous, protective response to limit ischaemic damage. Our previous report showed
365 increased levels of IL-1 β and NLRP3 expression after ischaemic stroke, but NLRP3 deficiency or
366 inhibition did not improve stroke outcome (Lemarchand et al., 2019). This could suggest that
367 endogenous itaconate production within the brain in response to ischaemia, whilst too late to inhibit
368 inflammatory cytokine production, may be able to limit NLRP3 inflammasome activation. It is
369 important to note that detection of increased NRF2 levels in response to DMI and 4OI treatment was
370 not reliable in the microglial models employed in this study, either due to a lower amount of NRF2
371 signalling, questioning the relevance of NRF2 activation in the brain, or due to the instability of NRF2
372 protein during OHSC sample processing steps such as water-bath sonication. It should also be noted
373 that the extent of NLRP3 inhibition mediated by the itaconate and fumarate derivatives in the OHSCs
374 was lower than in the BMDM and mixed glial assays. It is possible that higher doses or longer treatment
375 times of the metabolite derivatives would result in greater NLRP3 inhibition, given that we have
376 previously shown that MCC950 is able to potently inhibit IL-1 β release and ASC speck formation in
377 OHSCs (Hoyle et al., 2020).

378 We demonstrate that DMF, an approved clinical treatment for relapsing-remitting multiple sclerosis
379 (Fox et al., 2012; Gold et al., 2012b; Linker et al., 2011) and psoriasis (Smith, 2017), is an effective
380 NLRP3 inhibitor in both macrophages and microglia, as has been suggested previously (Garstekiewicz
381 et al., 2017; Liu et al., 2016; Miglio et al., 2015). We also show that DMF, as well as DMI and 4OI,
382 limits NLRP3 activation in response to LPC stimulation of macrophages, a demyelinating agent that
383 can drive NLRP3 and NLRC4 activation in macrophages, microglia and astrocytes (Freeman et al.,
384 2017). The mechanism underlying DMF's beneficial effect in multiple sclerosis and psoriasis is
385 unclear, and is commonly suggested to be mediated via NRF2 activation, although NRF2-independent
386 effects are also reported (Schulze-Topphoff et al., 2016). Given that DMF is able to potently inhibit
387 NLRP3 activation and directly inhibit gasdermin D cleavage (Humphries et al., 2020), and that NLRP3
388 is detrimental in the experimental autoimmune encephalomyelitis model of multiple sclerosis (Coll et
389 al., 2015; Gris et al., 2010; Jha et al., 2010), it is possible that DMF's protective response in multiple
390 sclerosis is in part mediated through dampened microglial and macrophage NLRP3 activation that may
391 promote or result from neuronal demyelination. Inhibition of NLRP3 activation in macrophages or
392 microglia could also facilitate other inflammatory responses that promote clearance of damaged myelin
393 and remyelination (Cunha et al., 2020). Evidence of caspase-1 activation and gasdermin D-mediated
394 pyroptosis has also been observed in the CNS of multiple sclerosis patients and in animal models (Li
395 et al., 2019; McKenzie et al., 2018), further implicating NLRP3 involvement. Upon administration,
396 DMF is hydrolysed to MMF and can be detected in the serum (Gold et al., 2012a; Litjens et al., 2004).
397 MMF also induces KEAP1 cysteine alkylation and NRF2 activation (Linker et al., 2011), suggesting
398 it may exert similar inhibitory effects to DMF on the priming response. Importantly, here we confirm
399 that MMF can inhibit NLRP3 activation in response to both nigericin and LPC stimulation in
400 macrophages, suggesting that NLRP3 inhibition could indeed be a relevant *in vivo* mechanism for DMF
401 treatment. While DMF exhibited toxic effects during the pre-treatment experiments, as its dose was
402 matched to that of 4OI, it is likely that titration of the DMF concentration would result in reduced
403 toxicity but similar potency. Given that DMI and 4OI, which both also drive NRF2 accumulation,
404 exerted similar inhibitory effects on nigericin- and LPC-induced NLRP3 activation, it is possible that
405 these itaconate derivatives may also offer therapeutic potential in the treatment of multiple sclerosis.
406 Indeed, DMI was recently shown to be protective in a mouse model of multiple sclerosis (Kuo et al.,
407 2020a).

408 We have revealed a two-pronged immunometabolic mechanism of NLRP3 regulation by limiting both
409 NLRP3 priming and canonical activation, suggesting that treatment with derivatives of metabolites

410 such as itaconate and fumarate may represent a viable therapeutic strategy in NLRP3-driven diseases,
411 although further work is required to confirm this. Future work should also aim to establish whether
412 itaconate and fumarate derivatives inhibit NLRP3 activation through the same or differing
413 mechanisms, either confirming this as a promising therapeutic target for drug design, or revealing novel
414 targets.

415 **4 Materials and methods**

416 *Mice*

417 In-house colonies of wild-type (WT) and ASC–citrine (Tzeng et al., 2016) C57BL/6 mice at the
418 University of Manchester were maintained to provide primary cell cultures. Animals were allowed free
419 access to food and water and maintained under temperature-, humidity- and light-controlled conditions.
420 All animal procedures adhered to the UK Animals (Scientific Procedures) Act (1986).

421 *Primary murine BMDM preparation*

422 Primary bone marrow-derived macrophages (BMDMs) were prepared by centrifuging the femurs of
423 3–6-month-old WT or ASC–citrine mice of either sex in an Eppendorf tube containing phosphate-
424 buffered saline (PBS) at $10,000 \times g$ (10 s). Bone marrow was collected and red blood cells were lysed
425 with ACK lysing buffer (Lonza, LZ10-548E). Cells were passed through a cell strainer (70 μm pore
426 size; Corning, 734-2761), centrifuged at $1500 \times g$ (5 min), and BMDMs were generated by
427 resuspending and culturing the cell pellet in 70% Dulbecco’s modified Eagle’s medium (DMEM;
428 Sigma, D6429) containing 10% (v/v) foetal bovine serum (FBS; Thermo, 10500064), 100
429 U ml^{-1} penicillin and 100 $\mu g ml^{-1}$ streptomycin (PenStrep; Thermo, 15070063), and supplemented
430 with 30% L929 mouse fibroblast-conditioned medium for 7 days. Cells were incubated at 37°C, 90%
431 humidity and 5% CO₂. Before experiments, BMDMs were seeded overnight at a density of $1 \times$
432 $10^6 ml^{-1}$.

433 *Human monocyte-derived macrophage preparation*

434 Human monocyte-derived macrophages (MDMs) were prepared from human peripheral blood
435 mononuclear cells (PBMCs) obtained from consenting healthy donors (National Health Service Blood
436 and Transplant, Manchester, UK), with full ethical approval from the University Research Ethics
437 Committee at the University of Manchester (ref 2017-2551-3945). In brief, PBMCs were isolated by

438 Ficoll separation (Thermo) at $400 \times g$ (40 min, room temperature) with zero deceleration. PBMCs were
439 washed three times with sterile MACS buffer (0.5% (w/v) bovine serum albumin (BSA), 2 mM EDTA
440 in PBS) before positive selection of CD14 $^{+}$ monocytes by incubation with magnetic CD14 microbeads
441 (Miltenyi Biotec, 130-050-201) (15 min, 4°C) and elution using LS columns (Miltenyi Biotec, 130-
442 042-401). CD14 $^{+}$ monocytes were differentiated to MDMs by culturing for 7 days (at a concentration
443 of 1×10^6 cells ml $^{-1}$) in RPMI 1640 (Sigma, R8758) supplemented with 10% (v/v) FBS, PenStrep and
444 macrophage colony-stimulating factor (M-CSF, 0.5 ng ml $^{-1}$; Peprotech, 300-25) at 37°C, 90% humidity
445 and 5% CO $_{2}$. On day 3 of differentiation, cells were fed by the addition of fresh media containing M-
446 CSF (0.5 ng ml $^{-1}$). Before experiments, MDMs were seeded overnight at a density of 1×10^6 ml $^{-1}$.

447 *Primary murine mixed glial culture preparation*

448 Murine mixed glial cells were prepared from the brains of 2–4-day-old mice of either sex that were
449 killed by cervical dislocation, as described previously (Hoyle et al., 2020). The brains were isolated,
450 cerebral hemispheres dissected and the meninges removed. The remaining brain tissue was
451 homogenised in DMEM containing 10% (v/v) FBS and PenStrep via repeated trituration, then
452 centrifuged at $500 \times g$ for 10 min and the pellet was resuspended in fresh culture medium before being
453 incubated in a flask at 37°C, 90% humidity and 5% CO $_{2}$. After 5 days, the cells were washed, and fresh
454 medium was applied. The medium was subsequently replaced every 2 days. On day 12 of the culture,
455 the cells were seeded at 2×10^5 cells ml $^{-1}$ in 24-well plates and incubated for a further 2 days prior to
456 use.

457 *Organotypic hippocampal slice culture (OHSC) preparation*

458 Seven-day-old mouse pups of either sex were killed by cervical dislocation and the brains were
459 collected in PBS containing glucose (5 mg ml $^{-1}$). The hippocampi were dissected and placed on filter
460 paper, and 400 μ m slices were prepared using a McIlwain tissue chopper (Brinkman Instruments).
461 Hippocampal slices were collected and placed on 0.4 μ m Millicell culture inserts (Merck Millipore,
462 PICM03050), as described previously by Stoppini et al. (1991). Three hippocampal slices were placed
463 on each insert. Slices were maintained in a humidified incubator with 5% CO $_{2}$ at 37°C with 1 ml MEM
464 (Gibco, 31095209) containing 20% (v/v) horse serum (Sigma, H1138), supplemented with HEPES
465 (30 mM; Fisher, 10397023) and insulin (0.1 mg ml $^{-1}$; Gibco, 12585014), pH 7.2–7.3. The culture
466 medium was changed every 2 days and slices were used at day 7.

467 *Treatment protocols*

468 To assess the effect of itaconate and fumarate derivative pre-treatments on inflammasome priming,
469 cells were first treated with vehicle (DMSO), DMI (Sigma, 592498), 4OI (Cayman Chemical,
470 CAY25374) or DMF (all 125 μ M; Sigma, 242926) for 20 h (BMDM) or 21 h (mixed glia and OHSC).
471 LPS (1 μ g ml $^{-1}$; Sigma, L2654) was then added to the wells for 4 h (BMDM) or 3 h (mixed glia and
472 OHSC) to induce priming, followed by nigericin (10 μ M; Sigma, N7143) for 60 min (BMDM and
473 mixed glia) or 90 min (OHSC) to activate the NLRP3 inflammasome.

474 To assess the direct effect of itaconate and fumarate derivative treatments on canonical NLRP3
475 inflammasome activation in macrophages, BMDMs and human MDMs were first primed with LPS
476 (1 μ g ml $^{-1}$) for 4 h. The medium was then replaced with serum-free DMEM (BMDM) or RPMI (human
477 MDM) containing vehicle (DMSO), DMI, 4OI, DMF (all 125 μ M, 15 min), MMF (500 μ M, 15 min
478 Sigma, 651419), exogenous itaconate (1–7.5 mM, 15 min; Sigma, I29204) or the NLRP3 inhibitor
479 MCC950 (10 μ M, 15 min; Sigma, PZ0280), before nigericin (10 μ M, 60 min) or LPC (100 μ M in
480 ethanol, 60 min; Sigma, L4129) was added to the culture medium. To assess the direct effect of
481 itaconate and fumarate derivative treatments on NLRP3 inflammasome activation in mixed glia and
482 OHSCs, cells were first primed with LPS (1 μ g ml $^{-1}$) for 3 h. The medium was then replaced with
483 serum-free DMEM (mixed glia) or MEM (OHSC) containing vehicle (DMSO), DMI, 4OI, DMF
484 (125 μ M, 15 min) or MMF (500 μ M, 15 min), before nigericin (10 μ M) was added to the culture
485 medium for 60 min (mixed glia) or 90 min (OHSC). At the end of the experiments, the supernatants
486 were collected and cell or OHSC lysates prepared for further analysis.

487 *Western blotting*

488 Primary BMDMs, mixed glia and OHSCs were lysed with lysis buffer (50 mM Tris/HCl, 150 mM
489 NaCl, Triton-X-100 1% v/v, pH 7.3) containing protease inhibitor cocktail (Merck Millipore, 539131).
490 OHSCs were additionally lysed using repeated trituration and brief water bath sonication. Lysates were
491 then centrifuged for 10 min at 12,000 \times g at 4°C. In experiments where cells were lysed in-well to
492 assess total protein content, cells were lysed by adding protease inhibitor cocktail and Triton-X-100
493 1% (v/v) into the culture medium. In-well lysates were concentrated by mixing with an equal volume
494 of trichloroacetic acid (Fisher, 10391351) and centrifuged for 10 min at 18,000 \times g at 4°C. The
495 supernatant was discarded, and the pellet resuspended in acetone (100%) before centrifugation for 10
496 min at 18,000 \times g at 4°C. The supernatant was again removed and the pellet allowed to air dry, before

497 resuspending in Laemmli buffer (2X). Samples were analysed for NRF2, pro-IL-1 β , mature IL-1 β ,
498 NLRP3, pro-caspase-1, caspase-1 p10, and gasdermin D. Equal amounts of protein from lysates or
499 equal volumes of in-well lysates were loaded into the gel. Samples were run on SDS-polyacrylamide
500 gels and transferred at 25 V onto nitrocellulose or PVDF membranes using a Trans-Blot[®] Turbo
501 TransferTM System (Bio-Rad). The membranes were blocked in either 5% w/v milk or 2.5% BSA
502 (Sigma, A3608) in PBS, 0.1% Tween 20 (PBST) for 1 h at room temperature. The membranes were
503 then washed with PBST and incubated at 4°C overnight with goat anti-mouse IL-1 β (250 ng ml⁻¹; R&D
504 Systems, AF-401-NA), mouse anti-mouse NLRP3 (1 μ g ml⁻¹; Adipogen, G-20B-0014-C100), rabbit
505 anti-mouse caspase-1 (1.87 μ g ml⁻¹; Abcam, ab179515), rabbit anti-mouse gasdermin D (0.6 μ g ml⁻¹;
506 Abcam, ab209845) or rabbit anti-mouse NRF2 (1.5 μ g ml⁻¹; CST, 12721) primary antibodies in 0.1%
507 (IL-1 β), 1% (NLRP3) or 2.5% (caspase-1, gasdermin D, NRF2) BSA in PBST. The membranes were
508 washed and incubated with rabbit anti-goat IgG (500 ng ml⁻¹, 5% milk in PBST; Dako, P044901-2),
509 rabbit anti-mouse IgG (1.3 μ g ml⁻¹, 5% milk in PBST; Dako, P026002-2) or goat anti-rabbit IgG
510 (250 ng ml⁻¹, 2.5% BSA in PBST; Dako, (Dako, P044801-2) at room temperature for 1 h. Proteins
511 were then visualised with Amersham ECL Western Blotting Detection Reagent (GE Healthcare,
512 RPN2236) and G:BOX (Syngene) and Genesys software. β -Actin (Sigma, A3854) was used as a
513 loading control. Densitometry was performed using FIJI (ImageJ). Uncropped western blots are
514 provided in Supplementary Figures 7-11.

515 *ELISA*

516 The levels of IL-1 β , IL-6 and tumour necrosis factor (TNF) in the supernatant were analysed by
517 enzyme-linked immunosorbent assay (ELISA; DuoSet, R&D systems) according to the manufacturer's
518 instructions.

519 *Cell death assays*

520 Cell death was assessed by measuring lactate dehydrogenase (LDH) release into the supernatant using
521 a CytoTox 96 Non-Radioactive Cytotoxicity Assay (Promega) according to the manufacturer's
522 instructions. Cell death in OHSCs was assessed by adding propidium iodide (25 μ g ml⁻¹; Sigma,
523 P4864) to the culture medium for the final 30 min of the inflammasome activation protocol followed
524 by widefield microscopy.

525 *Live imaging of ASC speck formation*

526 ASC-citrine-expressing primary BMDMs were used to perform live imaging of ASC speck formation.
527 For itaconate derivative pre-treatment assays, cells were seeded at 1×10^6 cells ml $^{-1}$ in 96-well plates
528 and incubated for 1 h, and were then treated with vehicle (DMSO), DMI, 4OI or DMF (125 μ M, 20 h).
529 LPS (1 μ g ml $^{-1}$, 4 h) was then added to the wells to induce priming. The medium was replaced with
530 optimem, and nigericin (10 μ M) was added to activate the NLRP3 inflammasome. For assays where
531 itaconate derivative treatments were added after LPS priming, cells were seeded overnight at 1×10^6
532 cells ml $^{-1}$ in 96-well plates. Cells were then first primed with LPS (1 μ g ml $^{-1}$, 4 h). The medium was
533 replaced with optimum containing vehicle, DMI, 4OI or DMF (125 μ M, 15 min) prior to addition of
534 nigericin (10 μ M). Image acquisition began immediately after nigericin treatment. Images were
535 subsequently acquired every 10 min for a further 90 min using an IncuCyte ZOOM $^{\circ}$ Live Cell Analysis
536 system (Essen Bioscience) at 37 $^{\circ}$ C using a 20X/0.61 S Plan Fluor objective. Speck number was
537 quantified using IncuCyte ZOOM $^{\circ}$ software, and was assessed for each treatment at the final time
538 point of 90 min.

539 *OHSC immunostaining*

540 OHSCs were washed once with cold PBS and fixed in 4% paraformaldehyde (1 h) at 4 $^{\circ}$ C. OHSCs
541 were washed two more times in cold PBS and then incubated with rabbit anti-mouse ASC (202 ng ml $^{-1}$;
542 CST, 67824) primary antibody overnight at 4 $^{\circ}$ C. OHSCs were washed and incubated with Alexa
543 Fluor $^{\text{TM}}$ 488 donkey anti-rabbit IgG (2 μ g ml $^{-1}$; Invitrogen, A-21206) secondary antibody for 2 h at
544 room temperature. All antibody incubations were performed using PBS, 0.3% Triton X-100. Wash
545 steps were performed using PBST unless stated otherwise. OHSCs were washed and then incubated in
546 DAPI (1 μ g ml $^{-1}$, 15 min; Sigma, D9542) at room temperature before final washing and mounting
547 using ProLong $^{\text{TM}}$ gold antifade mountant (Thermo, P36934) prior to imaging using widefield
548 microscopy.

549 *Snapshot widefield microscopy*

550 Images were collected on a Zeiss Axioimager.M2 upright microscope using a 5X or 20X Plan
551 Apochromat objective and captured using a Coolsnap HQ2 camera (Photometrics) through
552 Micromanager software (v1.4.23). Specific band-pass filter sets for DAPI and FITC were using to
553 prevent bleed-through from one channel to the next.

554 *Image processing analysis*

555 Analysis was performed using FIJI (ImageJ) on images acquired from the same region of up to three
556 separate OHSCs (from the same insert) per treatment, and these values were averaged for each
557 biological repeat. ASC speck formation was quantified on 20X widefield microscopy images by
558 subtracting background (50 pixel rolling ball radius), manually setting thresholds and analysing
559 particles with the following parameters: size 1–10 μm^2 , circularity 0.9–1.0. To quantify PI uptake,
560 images were acquired on a widefield microscope using a 5X objective, background was subtracted (5.0
561 pixel rolling ball radius) and thresholds for images were automatically determined using the default
562 method. The total area of PI-positive signal was measured in the whole field of view, and was then
563 normalised to the total area of DAPI signal.

564 *Data analysis*

565 Data are presented as the mean \pm standard error of the mean (SEM) together with individual data points
566 where possible. Data were analysed using repeated-measures one-way or two-way analysis of variance
567 (ANOVA), or mixed effects model, with Dunnett's or Sidak's post-hoc test using GraphPad Prism
568 (v8). Transformations or corrections were applied as necessary to obtain equal variance between groups
569 prior to analysis. Statistical significance was accepted at * $P<0.05$.

570 **5 Acknowledgments**

571 ASC-citrine mice were a kind gift from Douglas Golenbock (University of Massachusetts Medical
572 School) and Te-Chen Tzeng (Bristol Myers-Squibb, Cambridge, USA). We thank Dr Kevin Stacey
573 (University of Manchester) for the routine isolation of human PBMCs.

574 **6 Competing interests**

575 The authors declare that the research was conducted in the absence of any commercial or financial
576 relationships that could be construed as a potential conflict of interest.

577 **7 Funding**

578 This work was funded by the MRC (Grant No. MR/N003586/1 to DB and SMA, and MR/T011651/1
579 to DB) and was also funded by an MRC PhD studentship to CH (Grant No. MR/N013751/1). The
580 Bioimaging Facility microscopes used in this study were purchased with grants from BBSRC,
581 Wellcome Trust and the University of Manchester Strategic Fund.

582 **8 Data availability**

583 The data that support the findings of this study are available from the corresponding author upon
584 reasonable request.

585 **9 Author Contributions**

586 Conceptualisation: CH, EL, SMA and DB. Methodology: CH, EL and DB. Investigation: CH, EL and
587 JPG. Writing - original draft preparation: CH. Writing - review and editing: CH, EL, SMA and DB.
588 Visualisation: CH. Supervision: EL, SMA and DB. Funding acquisition: DB and SMA.

589 **10 References**

590 **Bambouskova, M., Gorvel, L., Lampropoulou, V., Sergushichev, A., Loginicheva, E., Johnson,**
591 **K., Korenfeld, D., Mathyer, M. E., Kim, H., Huang, L. H., et al.** (2018). Electrophilic
592 properties of itaconate and derivatives regulate the $\text{I}\kappa\text{B}\zeta$ -ATF3 inflammatory axis. *Nature* **556**,
593 501–504.

594 **Boucher, D., Monteleone, M., Coll, R. C., Chen, K. W., Ross, C. M., Teo, J. L., Gomez, G. A.,**
595 **Holley, C. L., Bierschenk, D., Stacey, K. J., et al.** (2018). Caspase-1 self-cleavage is an
596 intrinsic mechanism to terminate inflammasome activity. *J. Exp. Med.* **215**, 827–840.

597 **Chausse, B., Lewen, A., Poschet, G. and Kann, O.** (2020). Selective inhibition of mitochondrial
598 respiratory complexes controls the transition of microglia into a neurotoxic phenotype in situ.
599 *Brain. Behav. Immun.* **S0889-1591**, 30209–9.

600 **Chen, J. and Chen, Z. J.** (2018). PtdIns4P on dispersed trans-Golgi network mediates NLRP3
601 inflammasome activation. *Nature* **564**, 71–76.

602 **Chen, G. Y. and Nuñez, G.** (2010). Sterile inflammation: Sensing and reacting to damage. *Nat. Rev.*
603 *Immunol.* **10**, 826–837.

604 **Coll, R. C., Robertson, A. A., Chae, J. J., Higgins, S. C., Muñoz-Planillo, R., Inserra, M. C.,**
605 **Vetter, I., Dungan, L. S., Monks, B. G., Stutz, A., et al.** (2015). A small molecule inhibitor of
606 the NLRP3 inflammasome for the treatment of inflammatory diseases. *Nat Med* **21**, 248–255.

607 **Cunha, M. I., Su, M., Cantuti-Castelvetro, L., Müller, S. A., Schifferer, M., Djannatian, M.,**
608 **Alexopoulos, I., van der Meer, F., Winkler, A., van Ham, T. J., et al.** (2020). Pro-
609 inflammatory activation following demyelination is required for myelin clearance and
610 oligodendrogenesis. *J. Exp. Med.* **217**, e20191390.

611 **Dostert, C., Pétrilli, V., Van Bruggen, R., Steele, C., Mossman, B. T. and Tschopp, J.** (2008).
612 Innate Immune Activation Through Nalp3 Inflammasome Sensing of Asbestos and Silica.
613 *Science*. **320**, 674–677.

614 **ElAzzouny, M., Tom, C. T. M. B., Evans, C. R., Olson, L. L., Tanga, M. J., Gallagher, K. A.,**

615 **Martin, B. R. and Burant, C. F.** (2017). Dimethyl itaconate is not metabolized into itaconate
616 intracellularly. *J. Biol. Chem.* **292**, 4766–4769.

617 **Fox, R. J., Miller, D. H., Phillips, J. T., Hutchinson, M., Havrdova, E., Kita, M., Yang, M.,**

618 Raghupathi, K., Novas, M., Sweetser, M. T., et al.

619 (2012). Placebo-Controlled Phase 3 Study of Oral BG-12 or Glatiramer in Multiple Sclerosis. *N. Engl. J. Med.* **367**, 1087–1097.

620 **Freeman, L., Guo, H., David, C. N., Brickey, W. J., Jha, S. and Ting, J. P. Y.** (2017). NLR
621 members NLRC4 and NLRP3 mediate sterile inflammasome activation in microglia and
622 astrocytes. *J. Exp. Med.* **214**, 1351–1370.

623 **Gaidt, M. M., Ebert, T. S., Chauhan, D., Schmidt, T., Schmid-Burgk, J. L., Rapino, F.,**

624 Robertson, A. A. B., Cooper, M. A., Graf, T. and Hornung, V. (2016). Human Monocytes
625 Engage an Alternative Inflammasome Pathway. *Immunity* **44**, 833–846.

626 **Garstkiewicz, M., Strittmatter, G. E., Grossi, S., Sand, J., Fenini, G., Werner, S., French, L. E.,**
627 and Beer, H. D. (2017). Opposing effects of Nrf2 and Nrf2-activating compounds on the
628 NLRP3 inflammasome independent of Nrf2-mediated gene expression. *Eur. J. Immunol.* **47**,
629 806–817.

630 **Gold, R., Linker, R. A. and Stangel, M.** (2012a). Fumaric acid and its esters: An emerging
631 treatment for multiple sclerosis with antioxidative mechanism of action. *Clin. Immunol.* **142**,
632 44–48.

633 **Gold, R., Kappos, L., Arnold, D. L., Bar-Or, A., Giovannoni, G., Selmaj, K., Tornatore, C.,**

634 Sweetser, M. T., Yang, M., Sheikh, S. I., et al.

635 (2012b). Placebo-Controlled Phase 3 Study of Oral BG-12 for Relapsing Multiple Sclerosis. *N. Engl. J. Med.* **367**, 1098–1107.

636 **Gris, D., Ye, Z., Iocca, H. A., Wen, H., Craven, R. R., Gris, P., Huang, M., Schneider, M.,**
637 Miller, S. D. and Ting, J. P.-Y. (2010). NLRP3 plays a critical role in the development of
638 experimental autoimmune encephalomyelitis by mediating Th1 and Th17 responses. *J.*
639 *Immunol.* **185**, 974–81.

640 **Groß, C. J., Mishra, R., Schneider, K. S., Médard, G., Wettmarshausen, J., Dittlein, D. C., Shi,**
641 H., Gorka, O., Koenig, P.-A., Fromm, S., et al.

642 (2016). K⁺ Efflux-Independent NLRP3 Inflammasome Activation by Small Molecules Targeting Mitochondria. *Immunity* **45**, 761–773.

643 **Hall, S. M.** (1972). The Effect of Injections of Lysophosphatidyl Choline into White Matter of the
644 Adult Mouse Spinal Cord. *J. Cell Sci.* **10**,

645 **Halle, A., Hornung, V., Petzold, G. C., Stewart, C. R., Monks, B. G., Reinheckel, T., Fitzgerald,**
646 K. A., Latz, E., Moore, K. J. and Golenbock, D. T.

647 (2008). The NALP3 inflammasome is involved in the innate immune response to amyloid-beta. *Nat Immunol* **9**, 857–865.

648 **He, W.-T., Wan, H., Hu, L., Chen, P., Wang, X., Huang, Z., Yang, Z.-H., Zhong, C.-Q. and**
649 Han, J.

650 (2015). Gasdermin D is an executor of pyroptosis and required for interleukin-1 β secretion. *Cell Res.* **25**, 1285–98.

651 **Hooftman, A., Angiari, S., Hester, S., Corcoran, S. E., Runtsch, M. C., Ling, C., Ruzek, M. C.,**
652 Slivka, P. F., McGettrick, A. F., Banahan, K., et al.

653 (2020). The Immunomodulatory

653 Metabolite Itaconate Modifies NLRP3 and Inhibits Inflammasome Activation. *Cell Metab.* **32**,
654 468-478.e7.

655 **Hornung, V., Bauernfeind, F., Halle, A., Samstad, E. O., Kono, H., Rock, K. L., Fitzgerald, K.**
656 **A. and Latz, E.** (2008). Silica crystals and aluminum salts activate the NALP3 inflammasome
657 through phagosomal destabilization. *Nat. Immunol.* **9**, 847–856.

658 **Hoyle, C., Redondo-Castro, E., Cook, J., Tzeng, T., Allan, S. M., Brough, D. and Lemarchand,**
659 **E.** (2020). Hallmarks of NLRP3 inflammasome activation are observed in organotypic
660 hippocampal slice culture. *Immunology* imm.13221.

661 **Humphries, F., Shmuel-Galia, L., Ketelut-Carneiro, N., Li, S., Wang, B., Nemmara, V. V.,**
662 **Wilson, R., Jiang, Z., Khalighinejad, F., Muneeruddin, K., et al.** (2020). Succination
663 inactivates gasdermin D and blocks pyroptosis. *Science* (80-.). **369**, 1633–1637.

664 **Jha, S., Srivastava, S. Y., Brickey, W. J., Iocca, H., Toews, A., Morrison, J. P., Chen, V. S.,**
665 **Gris, D., Matsushima, G. K. and Ting, J. P. Y.** (2010). The inflammasome sensor, NLRP3,
666 regulates CNS inflammation and demyelination via caspase-1 and interleukin-18. *J. Neurosci.*
667 **30**, 15811–15820.

668 **Kayagaki, N., Warming, S., Lamkanfi, M., Walle, L. Vande, Louie, S., Dong, J., Newton, K.,**
669 **Qu, Y., Liu, J., Heldens, S., et al.** (2011). Non-canonical inflammasome activation targets
670 caspase-11. *Nature* **479**, 117–121.

671 **Kobayashi, E. H., Suzuki, T., Funayama, R., Nagashima, T., Hayashi, M., Sekine, H., Tanaka,**
672 **N., Moriguchi, T., Motohashi, H., Nakayama, K., et al.** (2016). Nrf2 suppresses macrophage
673 inflammatory response by blocking proinflammatory cytokine transcription. *Nat. Commun.* **7**,
674 11624.

675 **Kornberg, M. D., Bhargava, P., Kim, P. M., Putluri, V., Snowman, A. M., Putluri, N.,**
676 **Calabresi, P. A. and Snyder, S. H.** (2018). Dimethyl fumarate targets GAPDH and aerobic
677 glycolysis to modulate immunity. *Science* (80-.). **360**, 449–453.

678 **Kuo, P. C., Weng, W. T., Scofield, B. A., Paraiso, H. C., Brown, D. A., Wang, P. Y., Yu, I. C.**
679 **and Yen, J. H.** (2020a). Dimethyl itaconate, an itaconate derivative, exhibits
680 immunomodulatory effects on neuroinflammation in experimental autoimmune
681 encephalomyelitis. *J. Neuroinflammation* **17**,

682 **Kuo, P.-C., Weng, W.-T., Scofield, B. A., Furnas, D., Paraiso, H. C., Yu, I.-C. and Yen, J.-H.**
683 **(2020b).** Induction of IRG1 following ischemic stroke promotes HO-1 and BDNF expression to
684 alleviate neuroinflammation and restrain ischemic brain injury. *J. Neuroinflammation*.

685 **Lassmann, H. and Bradl, M.** (2017). Multiple sclerosis: experimental models and reality. *Acta*
686 *Neuropathol.* **133**, 223–244.

687 **Law, S. H., Chan, M. L., Marathe, G. K., Parveen, F., Chen, C. H. and Ke, L. Y.** (2019). An
688 updated review of lysophosphatidylcholine metabolism in human diseases. *Int. J. Mol. Sci.* **20**,
689 1149.

690 **Lemarchand, E., Barrington, J., Chenery, A., Haley, M., Coutts, G., Allen, J. E., Allan, S. M.**

691 **and Brough, D.** (2019). Extent of Ischemic Brain Injury After Thrombotic Stroke Is
692 Independent of the NLRP3 (NACHT, LRR and PYD Domains-Containing Protein 3)
693 Inflammasome. *Stroke* **50**, 1232–1239.

694 **Li, S., Wu, Y., Yang, D., Wu, C., Ma, C., Liu, X., Moynagh, P. N., Wang, B., Hu, G. and Yang, S.** (2019). Gasdermin D in peripheral myeloid cells drives neuroinflammation in experimental
695 autoimmune encephalomyelitis. *J. Exp. Med.* **216**, 2562–2581.

696

697 **Liao, S. T., Han, C., Xu, D. Q., Fu, X. W., Wang, J. S. and Kong, L. Y.** (2019). 4-Octyl itaconate
698 inhibits aerobic glycolysis by targeting GAPDH to exert anti-inflammatory effects. *Nat. Commun.* **10**, 5091.

699

700 **Linker, R. A., Lee, D. H., Ryan, S., Van Dam, A. M., Conrad, R., Bista, P., Zeng, W., Hronowsky, X., Buko, A., Chollate, S., et al.** (2011). Fumaric acid esters exert neuroprotective
701 effects in neuroinflammation via activation of the Nrf2 antioxidant pathway. *Brain* **134**, 678–
702 692.

703

704 **Litjens, N. H. R., Burggraaf, J., Van Strijen, E., Van Gulpen, C., Mattie, H., Schoemaker, R. C., Van Dissel, J. T., Thio, H. B. and Nibbering, P. H.** (2004). Pharmacokinetics of oral
705 fumarates in healthy subjects. *Br. J. Clin. Pharmacol.* **58**, 429–432.

706

707 **Liu, X., Zhou, W., Zhang, X., Lu, P., Du, Q., Tao, L., Ding, Y., Wang, Y. and Hu, R.** (2016).
708 Dimethyl fumarate ameliorates dextran sulfate sodium-induced murine experimental colitis by
709 activating Nrf2 and suppressing NLRP3 inflammasome activation. *Biochem. Pharmacol.* **112**,
710 37–49.

711

712 **Liu, L., Locascio, L. M. and Doré, S.** (2019). Critical Role of Nrf2 in Experimental Ischemic
713 Stroke. *Front. Pharmacol.* **10**, 153.

714

715 **McKenzie, B. A., Mamik, M. K., Saito, L. B., Boghozian, R., Monaco, M. C., Major, E. O., Lu, J. Q., Branton, W. G. and Power, C.** (2018). Caspase-1 inhibition prevents glial
716 inflammasome activation and pyroptosis in models of multiple sclerosis. *Proc. Natl. Acad. Sci. U. S. A.* **115**, E6065–E6074.

717

718 **Miglio, G., Veglia, E. and Fantozzi, R.** (2015). Fumaric acid esters prevent the NLRP3
719 inflammasome-mediated and ATP-triggered pyroptosis of differentiated THP-1 cells. *Int. Immunopharmacol.* **28**, 215–219.

720

721 **Mills, E. and O'Neill, L. A. J.** (2014). Succinate: A metabolic signal in inflammation. *Trends Cell Biol.* **24**, 313–320.

722

723 **Mills, E. L., Ryan, D. G., Prag, H. a., Dikovskaya, D., Menon, D., Zaslona, Z., Jedrychowski, M. P., Costa, A. S. H., Higgins, M., Hams, E., et al.** (2018). Itaconate is an anti-inflammatory
724 metabolite that activates Nrf2 via alkylation of KEAP1. *Nature* **556**, 113–117.

725

726 **Muñoz-Planillo, R., Kuffa, P., Martínez-Colón, G., Smith, B., Rajendiran, T. and Núñez, G.**
727 (2013). K⁺ Efflux Is the Common Trigger of NLRP3 Inflammasome Activation by Bacterial Toxins and Particulate Matter. *Immunity* **38**, 1142–1153.

728 **Nair, S., Huynh, J. P., Lampropoulou, V., Loginicheva, E., Esaulova, E., Gounder, A. P., Boon,**

729 **A. C. M., Schwarzkopf, E. A., Bradstreet, T. R., Edelson, B. T., et al.** (2018). Irg1 expression
730 in myeloid cells prevents immunopathology during *M. tuberculosis* infection. *J. Exp. Med.* **215**,
731 1035–1045.

732 **O'Neill, L. A. J. and Artyomov, M. N.** (2019). Itaconate: the poster child of metabolic
733 reprogramming in macrophage function. *Nat. Rev. Immunol.* **19**, 273–281.

734 **Olagnier, D., Farahani, E., Thyrsted, J., Blay-Cadanet, J., Herenget, A., Idorn, M., Hait, A.,**
735 **Hernaez, B., Knudsen, A., Iversen, M. B., et al.** (2020). SARS-CoV2-mediated suppression of
736 NRF2-signaling reveals potent antiviral and anti-inflammatory activity of 4-octyl-itaconate and
737 dimethyl fumarate. *Nat. Commun.* **11**, 4938.

738 **Perregaux, D. and Gabel, C. a.** (1994). Interleukin-1 β maturation and release in response to ATP
739 and nigericin. Evidence that potassium depletion mediated by these agents is a necessary and
740 common feature of their activity. *J. Biol. Chem.* **269**, 15195–15203.

741 **Pinteaux, E., Parker, L. C., Rothwell, N. J. and Luheshi, G. N.** (2002). Expression of interleukin-
742 1 receptors and their role in interleukin-1 actions in murine microglial cells. *J. Neurochem.* **83**,
743 754–763.

744 **Plemel, J. R., Michaels, N. J., Weishaupt, N., Caprariello, A. V., Keough, M. B., Rogers, J. A.,**
745 **Yukseloglu, A., Lim, J., Patel, V. V., Rawji, K. S., et al.** (2018). Mechanisms of
746 lysophosphatidylcholine-induced demyelination: A primary lipid disrupting myelinopathy. *Glia*
747 **66**, 327–347.

748 **Qin, W., Zhang, Y., Tang, H., Liu, D., Chen, Y., Liu, Y. and Wang, C.** (2020). Chemoproteomic
749 Profiling of Itaconation by Bioorthogonal Probes in Inflammatory Macrophages. *J. Am. Chem.*
750 *Soc.* **142**, 10894–10898.

751 **Rock, K. L., Latz, E., Ontiveros, F. and Kono, H.** (2010). The sterile inflammatory response.
752 *Annu. Rev. Immunol.* **28**, 321–42.

753 **Schaum, N., Karkanias, J., Neff, N. F., May, A. P., Quake, S. R., Wyss-Coray, T., Darmanis, S.,**
754 **Batson, J., Botvinnik, O., Chen, M. B., et al.** (2018). Single-cell transcriptomics of 20 mouse
755 organs creates a Tabula Muris. *Nature* **562**, 367–372.

756 **Schroder, K. and Tschopp, J.** (2010). The Inflammasomes. *Cell* **140**, 821–832.

757 **Schulze-Topphoff, U., Varrin-Doyer, M., Pekarek, K., Spencer, C. M., Shetty, A., Sagan, S. A.,**
758 **Cree, B. A. C., Sobel, R. A., Wipke, B. T., Steinman, L., et al.** (2016). Dimethyl fumarate
759 treatment induces adaptive and innate immune modulation independent of Nrf2. *Proc. Natl.*
760 *Acad. Sci. U. S. A.* **113**, 4777–4782.

761 **Seoane, P. I., Lee, B., Hoyle, C., Yu, S., Lopez-Castejon, G., Lowe, M. and Brough, D.** (2020).
762 The NLRP3-inflammasome as a sensor of organelle dysfunction. *J. Cell Biol.* **219**, e202006194.

763 **Sheppard, O., Coleman, M. P. and Durrant, C. S.** (2019). Lipopolysaccharide-induced
764 neuroinflammation induces presynaptic disruption through a direct action on brain tissue
765 involving microglia-derived interleukin 1 beta. *J. Neuroinflammation* **16**, 1–13.

766 **Smith, D.** (2017). Fumaric acid esters for psoriasis: a systematic review. *Ir. J. Med. Sci.* **186**, 161–
767 177.

768 **Stoppini, L., Buchs, P. and Muller, D.** (1991). A simple method for organotypic cultures of nervous
769 tissue. *J. Neurosci. Methods* **37**, 173–182.

770 **Swain, A., Bambouskova, M., Kim, H., Andhey, P. S., Duncan, D., Auclair, K., Chubukov, V.,**
771 **Simons, D. M., Roddy, T. P., Stewart, K. M., et al.** (2020). Comparative evaluation of
772 itaconate and its derivatives reveals divergent inflammasome and type I interferon regulation in
773 macrophages. *Nat. Metab.* 1–9.

774 **Tannahill, G., Curtis, A., Adamik, J., Palsson-McDermott, E., McGettrick, A., Goel, G., Frezza,**
775 **C., Bernard, N., Kelly, B., Foley, N., et al.** (2013). Succinate is an inflammatory signal that
776 induces IL-1 β via HIF-1 α . *Nature* **496**, 238–242.

777 **Trotter, A., Anstadt, E., Clark, R. B., Nichols, F., Dwivedi, A., Aung, K. and Cervantes, J. L.**
778 (2019). The role of phospholipase A2 in multiple Sclerosis: A systematic review and meta-
779 analysis. *Mult. Scler. Relat. Disord.* **27**, 206–213.

780 **Tzeng, T. C., Schattgen, S., Monks, B., Wang, D., Cerny, A., Latz, E., Fitzgerald, K. and**
781 **Golenbock, D. T.** (2016). A Fluorescent Reporter Mouse for Inflammasome Assembly
782 Demonstrates an Important Role for Cell-Bound and Free ASC Specks during In Vivo Infection.
783 *Cell Rep.* **16**, 571–582.

784 **Wilms, H., Sievers, J., Rickert, U., Rostami-Yazdi, M., Mrowietz, U. and Lucius, R.** (2010).
785 Dimethylfumarate inhibits microglial and astrocytic inflammation by suppressing the synthesis
786 of nitric oxide, IL-1 β , TNF- α and IL-6 in an in-vitro model of brain inflammation. *J.*
787 *Neuroinflammation* **7**, 30.

788 **Zhang, Y., Chen, K., Sloan, S. A., Bennett, M. L., Scholze, A. R., O'Keeffe, S., Phatnani, H. P.,**
789 **Guarnieri, P., Caneda, C., Ruderisch, N., et al.** (2014). An RNA-Sequencing Transcriptome
790 and Splicing Database of Glia, Neurons, and Vascular Cells of the Cerebral Cortex. *J. Neurosci.*
791 **34**, 11929–11947.

792